


# Extremely low frequency electromagnetic stimulation reduces ischemic stroke volume by improving cerebral collateral blood flow

Journal of Cerebral Blood Flow & Metabolism  
2022, Vol. 42(6) 979–996  
© The Author(s) 2022  
Article reuse guidelines:  
sagepub.com/journals-permissions  
DOI: 10.1177/0271678X221084410  
journals.sagepub.com/home/jcbfm



Hannelore Kemps<sup>1</sup>, Chantal Dessy<sup>2</sup>, Laurent Dumas<sup>2</sup>, Pierre Sonveaux<sup>2</sup>, Lotte Alders<sup>1</sup>, Jana Van Broeckhoven<sup>1</sup>, Lena Perez Font<sup>3</sup>, Sara Lambrichts<sup>4</sup>, Sébastien Foulquier<sup>4,5</sup>, Sven Hendrix<sup>1,6</sup>, Bert Brône<sup>1</sup> , Robin Lemmens<sup>7,8,9</sup> and Annelies Bronckaers<sup>1</sup>

## Abstract

Extremely low frequency electromagnetic stimulation (ELF-EMS) has been considered as a neuroprotective therapy for ischemic stroke based on its capacity to induce nitric oxide (NO) signaling. Here, we examined whether ELF-EMS reduces ischemic stroke volume by stimulating cerebral collateral perfusion. Moreover, the pathway responsible for ELF-EMS-induced NO production was investigated. ELF-EMS diminished infarct growth following experimental stroke in collateral-rich C57BL/6 mice, but not in collateral-scarce BALB/c mice, suggesting that decreased lesion sizes after ELF-EMS results from improved collateral blood flow. *In vitro* analysis demonstrated that ELF-EMS increased endothelial NO levels by stimulating the Akt-/eNOS pathway. Furthermore, ELF-EMS augmented perfusion in the hind limb of healthy mice, which was mediated by enhanced Akt-/eNOS signaling. In healthy C57BL/6 mouse brains, ELF-EMS treatment increased cerebral blood flow in a NOS-dependent manner, whereas no improvement in cerebrovascular perfusion was observed in collateral-sparse BALB/c mice. In addition, ELF-EMS enhanced cerebral blood flow in both the contra- and ipsilateral hemispheres of C57BL/6 mice subjected to experimental ischemic stroke. In conclusion, we showed that ELF-EMS enhances (cerebro)vascular perfusion by stimulating NO production, indicating that ELF-EMS could be an attractive therapeutic strategy for acute ischemic stroke by improving cerebral collateral blood flow.

## Keywords

Akt-/eNOS pathway, cerebral collateral blood flow, extremely low frequency electromagnetic stimulation, ischemic stroke, nitric oxide

Received 7 September 2021; Revised 3 February 2022; Accepted 4 February 2022

<sup>1</sup>Biomedical Research Institute (BIOMED), Hasselt University (UHasselt), Diepenbeek, Belgium

<sup>2</sup>Pole of Pharmacology and Therapeutics, Institut de Recherche Expérimentale et Clinique (IREC), Université catholique de Louvain (UCLouvain), Brussels, Belgium

<sup>3</sup>Centro Nacional de Electromagnetismo Aplicado (CNEA), Universidad de Oriente, Santiago de Cuba, Cuba

<sup>4</sup>Department of Pharmacology and Toxicology, School for Mental Health and Neuroscience, Maastricht University Medical Center+, Maastricht, The Netherlands

<sup>5</sup>CARIM, School for Cardiovascular Diseases, Maastricht University, Maastricht, The Netherlands

<sup>6</sup>Medical School Hamburg, Hamburg, Germany

<sup>7</sup>KU Leuven, – University of Leuven, Department of Neurosciences, Experimental Neurology, Leuven, Belgium

<sup>8</sup>VIB, Center for Brain & Disease Research, Laboratory of Neurobiology, Leuven, Belgium

<sup>9</sup>Department of Neurology, University Hospitals Leuven, Leuven, Belgium

## Corresponding author:

Annelies Bronckaers, Agoralaan Building C, 3590, Diepenbeek, Belgium.  
Email: annelies.bronckaers@uhasselt.be

## Introduction

Following cerebral ischemia, several endogenous repair processes are stimulated. In the acute phase after symptom onset, one of the main mechanisms to compensate for the reduced blood flow to the affected area is the recruitment of the leptomeningeal collateral circulation.<sup>1</sup> The ability of collateral recruitment is strongly associated with stroke outcome.<sup>2</sup> Accordingly, improving collateral perfusion is proposed to be a potent therapeutic option. The gaseous molecular messenger nitric oxide (NO) plays a crucial role in the induction of collateral blood flow.<sup>1</sup> Within the brain, NO is an important signaling molecule synthesized by three distinct isoforms of nitric oxide synthases (NOSs); neuronal NOS (nNOS), inducible NOS (iNOS), and endothelial NOS (eNOS).<sup>3,4</sup> After cerebral ischemia, the role of NO is rather complex.<sup>3,5</sup> On one hand, NO generated by nNOS and iNOS is detrimental for neuronal survival after stroke, due to production of the neurotoxic peroxynitrite.<sup>6,7</sup> On the other hand, eNOS derived NO induces angiogenesis and vasodilation, thereby being considered to act as a neuroprotective agent.<sup>3,5,8</sup> Concordantly, nNOS knockout mice displayed smaller lesion sizes and increased neurogenesis after ischemic stroke. In contrast, eNOS deficiency in mice resulted in larger infarcts and reduced neurogenesis compared to wild-type animals.<sup>8,9</sup> Hence, increasing post-ischemic NO content by upregulating eNOS activity is considered to be a putative treatment strategy for ischemic stroke.<sup>6</sup>

Recently, extremely low frequency electromagnetic stimulation (ELF-EMS) has been explored as a non-invasive therapy for a wide variety of neurological disorders, including traumatic brain injury, Huntington's disease, and ischemic stroke.<sup>10–13</sup> In the clinic, ELF-EMS is approved for the treatment of postoperative pain, delayed union bone fractures, edema, and chronic wounds.<sup>14–17</sup> Although the cellular and molecular mechanisms of ELF-EMS have not been fully elucidated, several reports indicated ELF-EMS to induce NO production.<sup>13,18–21</sup> In a rat model of global cerebral ischemia, we previously demonstrated that ELF-EMS improved survival rates and reduced infarct sizes, which was likely attributed to enhanced NO signaling.<sup>13</sup> However, the mechanism by which NO production is induced remains unknown.

In this study, we shed light on the (sub)cellular mechanisms underlying the effect of ELF-EMS on NO production. We postulated that ELF-EMS could reduce infarct growth by stimulating cerebral collateral blood flow via activation of eNOS-/NO signaling. First, the therapeutic response of ELF-EMS following ischemic stroke was examined in two different mouse strains with variations in their native collateral

circulation. Secondly, we investigated the role of the Akt-/eNOS pathway in the induction of endothelial NO production by ELF-EMS *in vitro*. Next, the potential of ELF-EMS to enhance blood perfusion by inducing Akt-/eNOS signaling was studied in the hind limbs of healthy mice. Furthermore, the effect of ELF-EMS on cerebral collateral blood flow and the involvement of NOS signaling herein was assessed. Finally, we evaluated whether ELF-EMS treatment could potentially reduce ischemia-induced brain damage by augmenting cerebral blood flow towards the infarcted tissue.

## Materials and methods

### Specifications of non-pulsed ELF-EMS

ELF-EMS was generated by using a coil (ferromagnetic core radius 16 mm; wire diameter 0.20 mm; 950 turns) connected to a Magnetic Stimulator NaK-02 and power amplifier (high fidelity amplifier; bandwidth 10 Hz–20 kHz; output 60 W) manufactured by our collaborators from Cuba (F.G. González, M.C. Cardonne and L.P. Font of Centro Nacional de Electromagnetismo Aplicado (CNEA)). The produced magnetic field was measured using a calibrated PCE-MFM 3000 gaussmeter (PCE Instruments, Enschede, The Netherlands). The resulting magnetic field generated a continuous sinusoidal current of 60 Hz with a magnetic intensity of 13.5 mT and was applied without intervals to deliver an electromagnetic field in a non-pulsed manner.<sup>13</sup>

### Animal experiments

Ten-week-old male C57BL/6 and BALB/c mice were obtained from Envigo (Horst, The Netherlands). Ten-week-old NMRI RjHan male mice were purchased from Janvier (Le Genest-Saint-Isle, France). In all experiments, animals were randomly assigned to either sham or ELF-EMS treatment using blocking randomisation. Mice were housed under standardized conditions with a 12 h light–dark cycle and a controlled temperature of  $20 \pm 3$  °C. Food and water were provided *ad libitum*. The experiments were performed according to the guidelines defined in the “Principles of laboratory animal care” (NIH publication No. 86-23, revised 1985), the EU Directive 2010/63/EU as well as the specific Belgian law (Belgian law of animal welfare and Royal Decree of 29 May 2013). All experiments were approved by the Ethical Committee for Animal Experimentation (ECAE) of Hasselt University or by the Institutional Animal Care and Research Advisory Committee of the Université catholique de Louvain (agreement # 2016/UCL/MD/017 and

2016/UCL/MD/018) and were reported in accordance with the ARRIVE 2.0 guidelines.<sup>22</sup>

### **Permanent distal middle cerebral artery occlusion (dMCAO)**

Ten-week-old male C57BL/6 and BALB/c mice were subjected to permanent dMCAO as described previously,<sup>23</sup> with minor modifications. Details regarding the surgical procedure are described in the supplemental materials.

Exactly 1 h after dMCAO, mice were anesthetized using ketamine/xylazine (ketamine: 120 mg/kg and xylazine: 10 mg/kg; intraperitoneal injection (IP)) and placed in a restrainer to receive treatment. Mice were exposed to either sham or ELF-EMS treatment (60 Hz, 13.5 mT) for 20 min over 4 consecutive days. Sham-treated mice were anesthetized and placed in the restrainer under the ELF-EMS device without exposure to the electromagnetic field. After 7 days, mice were sacrificed to analyze infarct size via 2,3,5-triphenyltetrazolium chloride (TTC) staining. Details regarding the TTC staining of brain sections are provided in the supplemental section.

### **Laser speckle contrast imaging (LSCI)**

Superficial cortical blood flow was assessed in 10-week-old male C57BL/6 and BALB/c mice using a full-field Laser Speckle Contrast imager (FLPI-2, Moor Instruments, Axminster, UK). Cerebral blood flow was measured in healthy C57BL/6 and BALB/c animals, as well as in C57BL/6 mice subjected to dMCAO 1 h and 24 h after stroke induction. To assess the role of NOS-/NO signaling in ELF-EMS-mediated effects on cerebrovascular perfusion, healthy 10-week-old male C57BL/6 mice were treated with L-NAME (1 g/500 ml; Sigma-Aldrich) supplemented to the drinking water for 5 subsequent days prior to Laser Speckle Contrast imaging. Details regarding the experimental set-up are described in the supplemental materials.

### **Laser doppler imaging**

Blood perfusion in the hind limbs of 10-week-old NMRI RjHan mice was measured using a Laser Doppler imager (Moor Instruments), as previously described.<sup>24</sup> More experimental details are specified in the supplemental materials.

For experiments with pathway inhibitors, 10-week-old male NMRI RjHan mice were pre-treated with either L-NAME (1 g/500 ml; Sigma-Aldrich), LY294002 (10 mg/kg, Cayman Chemical, Michigan, USA), ARL 17477 (10 mg/kg, Tocris Bioscience, Bristol, UK), or 1400 W (10 mg/kg, Cayman

Chemical). L-NAME was added to the drinking water for 5 subsequent days prior to Laser Doppler imaging. ARL 17477 and 1400 W were injected IP once a day for 6 days, whereas LY294002 was administered IP for 3 days once a day. The last injection was delivered 1 h prior to Laser Doppler imaging.

### **Nitrite measurements**

Cell culture methods of human microvascular endothelial cells (HMEC-1) are provided in the supplemental materials. To assess nitrite production, HMEC-1 were seeded at a density of  $78.95 \times 10^3$  cells/cm<sup>2</sup> in a 24-well plate. After adherence of the cells, 300  $\mu$ l fresh standard HMEC-1 culture medium was added. Prior to ELF-EMS treatment, pathway inhibitors were administered for 30 min in the case of L-NMMA (1.5 mM, Tocris Bioscience, IC50: 2.7  $\mu$ M)<sup>13</sup> and LY294002 (20  $\mu$ M, Sigma-Aldrich, IC50: 1.4  $\mu$ M)<sup>25</sup> or for 2 h in the case of 1400 W (3  $\mu$ M, Cayman Chemical, IC50: <0.2  $\mu$ M)<sup>26</sup> and ARL 17477 (5  $\mu$ M, Tocris Bioscience, IC50: 35 nM).<sup>27</sup> Cells were then either stimulated or not for 20 min with ELF-EMS (60 Hz, 13.5 mT). After 24 h, medium was collected, centrifuged and stored at  $-80^\circ\text{C}$ . Nitrite levels were measured using the Griess Reagent System (Promega Benelux B.V., Leiden, The Netherlands) according to manufacturer's guidelines.

### **Cyclic guanosine-3',5'-monophosphate (cGMP) enzyme-linked immunosorbent assay (ELISA)**

HMEC-1 were seeded at a density of  $78.95 \times 10^3$  cells/cm<sup>2</sup> in a 6-well plate. Cells were washed twice with FBS-free MCDB 131 medium supplemented with 10 mM L-glutamine and were incubated for 4 h with 2 ml FBS-free MCDB 131 medium containing 10 mM L-glutamine and 1 mM IBMX (Sigma-Aldrich). Prior to ELF-EMS, HMEC-1 were pre-treated with L-arginine (200  $\mu$ M, Tocris Bioscience) for 30 min. After 4 h, cells were either left unstimulated or treated with ELF-EMS for 20 min (60 Hz, 13.5 mT). Immediately after, HMEC-1 were lysed using 0.1 M HCl (VWR Chemicals, Leuven, Belgium) + 1% Triton (Sigma-Aldrich) at room temperature. Samples were centrifuged and stored at  $-80^\circ\text{C}$ . Protein concentration of lysed HMEC-1 was determined by the Pierce BCA assay kit (ThermoFisher Scientific, Erembodegem, Belgium). cGMP production was measured using the cGMP ELISA kit (Cayman Chemical) following manufacturer's instructions.

### **Small interfering RNA (siRNA) transfection**

ON-TARGETplus eNOS (NOS3) SMARTpool siRNA and ON-TARGETplus Non-targeting siRNA were purchased from Dharmacon (Boulder, USA).

siRNA sequences are listed in Supplementary Table 1. HMEC-1 were seeded in penicillin and streptomycin-free standard HMEC-1 culture medium at a density of  $20.83 \times 10^3$  cells/cm<sup>2</sup>. After 24 h, the cells were transfected with 50 nM siRNA using 4  $\mu$ l DharmaFECT™ Transfection Reagent (Dharmacon) per well according to manufacturer's guidelines. Medium was renewed 24 h after transfection and HMEC-1 were incubated for an additional 48 h, after which the cells were lysed for western blot analyses.

### Western blotting

Protein sample preparation methods are provided in the supplemental materials. Equal amounts of proteins (3–20  $\mu$ g) were diluted in 5X SDS loading buffer (10% SDS, 50% glycerol, 0.325 M Tris-HCl (pH 6.8), and 0.025% bromophenol blue) and electrophoretically separated on 10% SDS-PAGE gels. Proteins were transferred onto polyvinylidene fluoride membranes (Merck Millipore, Darmstadt, Germany) for 2 h at 350 mA. Membranes were blocked for 1 h at room temperature with 2% nonfat dry milk in phosphate buffered saline (PBS) containing 0.05% Tween-20 (PBS-T), followed by overnight incubation with primary antibodies at 4°C. Primary antibodies are listed in Supplementary Table 2. The following horseradish peroxidase (HRP)-conjugated secondary antibodies were then used for a 1 h incubation at room temperature: goat anti-rabbit HRP (P0448, Agilent, Heverlee, Belgium), rabbit anti-goat HRP (P0449, Agilent), and rabbit anti-mouse HRP (P0260, Agilent). All antibodies were diluted in 2% nonfat dry milk in PBS-T.  $\beta$ -actin was used as loading control. Pierce ECL Plus Western Blotting Substrate (ThermoFisher Scientific) was applied to the membranes for signal detection. Images were acquired with ImageQuant LAS 4000 Mini (GE Healthcare Bio-Sciences, Uppsala, Sweden). Densitometric analyses were performed with the use of ImageQuant™ TL LAS 4000 software (GE Healthcare Bio-Sciences).

### Statistical analysis

All statistical analyses were performed using Graphpad Prism 7.04 software (Graphpad, San Diego, CA, USA). Normality was tested using the D'Agostino and Pearson normality test. In case of normally distributed data, one sample T-test (comparison of 1 group to a hypothetical value), unpaired Student T-test (2 groups) or one-way ANOVA (3 or more groups) followed by Tukey multiple comparison test was performed. The nonparametric Mann-Whitney test (2 groups) or Kruskal-Wallis test (3 or more groups) following Dunn's multiple comparison test was used for data

that were not normally distributed. All data are displayed as mean  $\pm$  standard deviation (SD). A p-value of  $\leq 0.05$  was considered to be statistically significant.

## Results

### *ELF-EMS reduces infarct size after ischemic stroke in collateral-rich C57BL/6 mice, but not in collateral-scarce BALB/c mice*

Previously, our research group demonstrated that ELF-EMS application reduced lesion size in a rat model of global cerebral ischemia, which was likely mediated by enhanced NO signaling.<sup>13</sup> Since NO is a critical regulator of cerebral collateral blood flow,<sup>1</sup> we postulated that ELF-EMS exerts its protective effects following ischemic stroke by recruiting the collateral circulation. Hence, the therapeutic response of ELF-EMS after experimental stroke was investigated in two different mouse strains with variations in their native cerebral collateral circulation. BALB/c mice exhibit lower numbers of pial collaterals in comparison with C57BL/6 mice, which possess an extensive network of cerebral collaterals.<sup>28</sup> Mice were exposed to either sham or ELF-EMS treatment for 4 consecutive days after induction of ischemic stroke (Figure 1(a)). C57BL/6 mice subjected to dMCAO showed a reduction in infarct size by 24% after ELF-EMS treatment compared to sham-treated C57BL/6 mice ( $19 \pm 6$  mm<sup>3</sup> vs.  $25 \pm 6$  mm<sup>3</sup>) (Figure 1(b) and (c)). However, ELF-EMS treatment had no effect on lesion volume in the BALB/c mouse strain compared to sham-treated animals ( $40 \pm 13$  mm<sup>3</sup> vs.  $45 \pm 11$  mm<sup>3</sup>) (Figure 1(d) and (e)). Since BALB/c mice possess only a limited amount of cerebral collaterals and supposedly do not benefit from the protective effects of ELF-EMS, these results suggest that ELF-EMS reduces ischemic stroke volume by stimulating cerebral collateral blood flow.

### *ELF-EMS stimulates NO production in an eNOS-dependent manner*

Since the mechanisms by which ELF-EMS induces NO production remain unknown, we investigated the activated NO pathway in response to ELF-EMS *in vitro* using human microvascular endothelial cell lines (HMEC-1 and hCMEC/D3 cell lines). Ultrastructural analysis of ELF-EMS-treated HMEC-1 revealed no gross intracellular changes induced by the treatment (Supplementary Figure 1). ELF-EMS increased nitrite levels in both dermal-derived HMEC-1 ( $176 \pm 32\%$  for ELF-EMS-treated cells vs.  $100 \pm 20\%$  for control cells) (Figure 2(a)) and brain-derived hCMEC/D3 cells (Supplementary Figure 2) compared to unstimulated cells. In addition, production of cGMP, a downstream



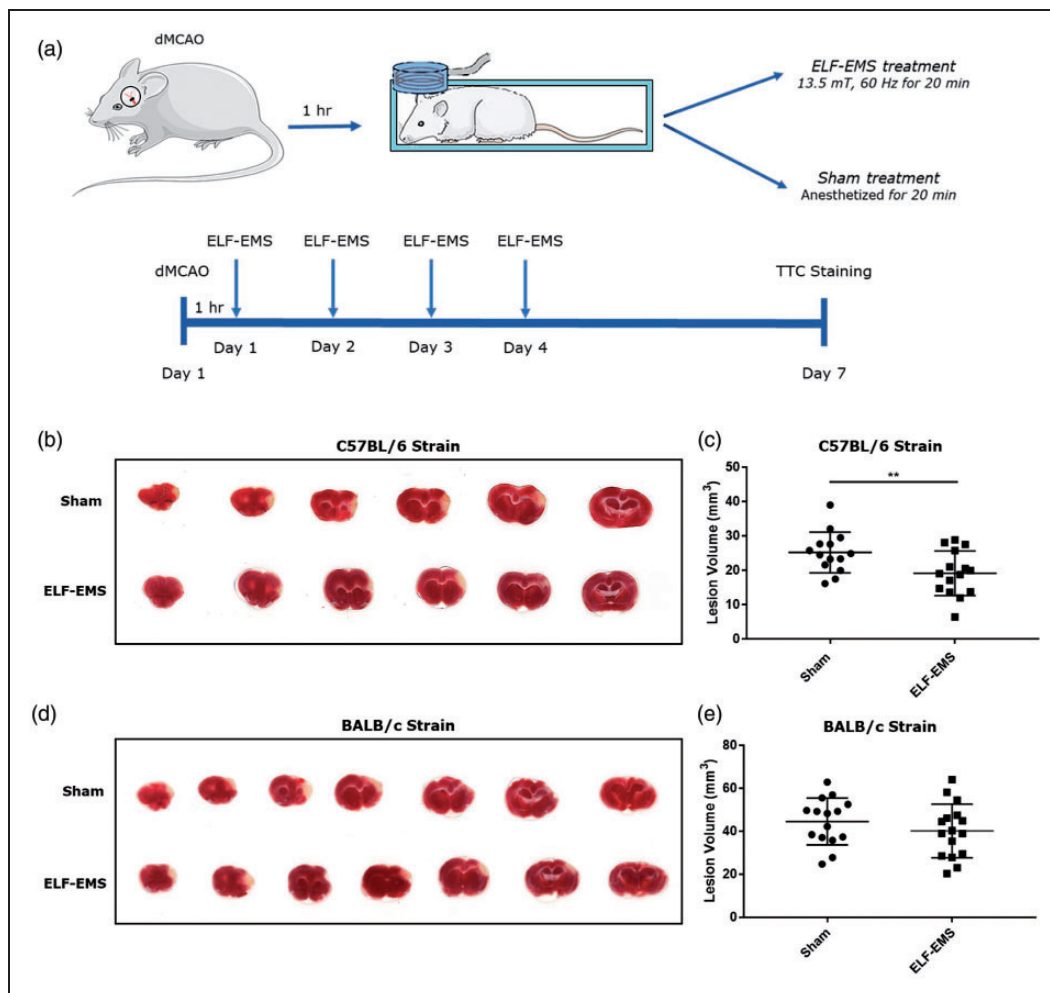


**Figure 1.** ELF-EMS treatment reduces ischemic stroke volume in C57BL/6 mice, but not in BALB/c mice. (a) Schematic overview of the experimental set-up. Infarct volume was assessed 7 days after dMCAO induction on brain slices stained with 2,3,5-triphenyltetrazolium chloride (TTC). The scheme was created using Servier Medical Art. (b) Representative images of TTC-stained brain slices of either sham or ELF-EMS-treated C57BL/6 mice. (c) Quantification of lesion volume on the acquired TTC images of C57BL/6 mice demonstrated a reduction in infarct size in the ELF-EMS-treated group. ( $n = 14$ ;  $p = 0.0072$ ). (d) Representative images of TTC-stained brain slices of either sham or ELF-EMS-treated BALB/c mice. (e) Quantification of lesion volume on the acquired TTC images of BALB/c mice showed no effect of ELF-EMS on lesion size. ( $n = 15$ ;  $p = 0.1539$ ). Data are represented as mean  $\pm$  SD. \*\* $p < 0.01$ .

signaling molecule in the NO cascade, was enhanced approximately 4-fold by ELF-EMS treatment ( $0.108 \pm 0.04$  pmol/mg vs.  $0.028 \pm 0.03$  pmol/mg) (Figure 2(b)). Pre-incubation of HMEC-1 with the pan-NOS inhibitor L-NMMA reduced ELF-EMS-induced nitrite levels to  $121 \pm 25\%$ , suggesting that the enhanced NO production by ELF-EMS is NOS-dependent (Figure 2(a)). To identify which NOS isoform is responsible for ELF-EMS-induced NO signaling, the protein levels of the three NOS isoforms were assessed in unstimulated and ELF-EMS-treated HMEC-1. Both control and ELF-EMS-stimulated HMEC-1 expressed eNOS, whereas nNOS and iNOS protein levels were negligible or not detectable (Supplementary Figure 3(a)). Since there are no

selective inhibitors available for eNOS, a selective iNOS inhibitor (1400 W) and a specific nNOS inhibitor (ARL 17477) were used to identify which NOS isoform is accountable for the increased NO production. Incubation of HMEC-1 with 1400 W and ARL 17477 did not influence ELF-EMS-induced nitrite production (Figure 2(c) and (d)), indicating that eNOS is the activated NOS isoform by ELF-EMS. Enhanced eNOS activation was confirmed by assessing its phosphorylation status. Phosphorylation of eNOS (peNOS) at Thr495 attenuates eNOS function, while phosphorylation at Ser1177 stimulates eNOS activity.<sup>29</sup> ELF-EMS increased eNOS phosphorylation on Ser1177 ( $181 \pm 84\%$  vs.  $100 \pm 110\%$ ) (Figure 2(e)) and decreased its phosphorylation on Thr495 ( $74 \pm 11\%$  vs.  $100 \pm 27\%$ )

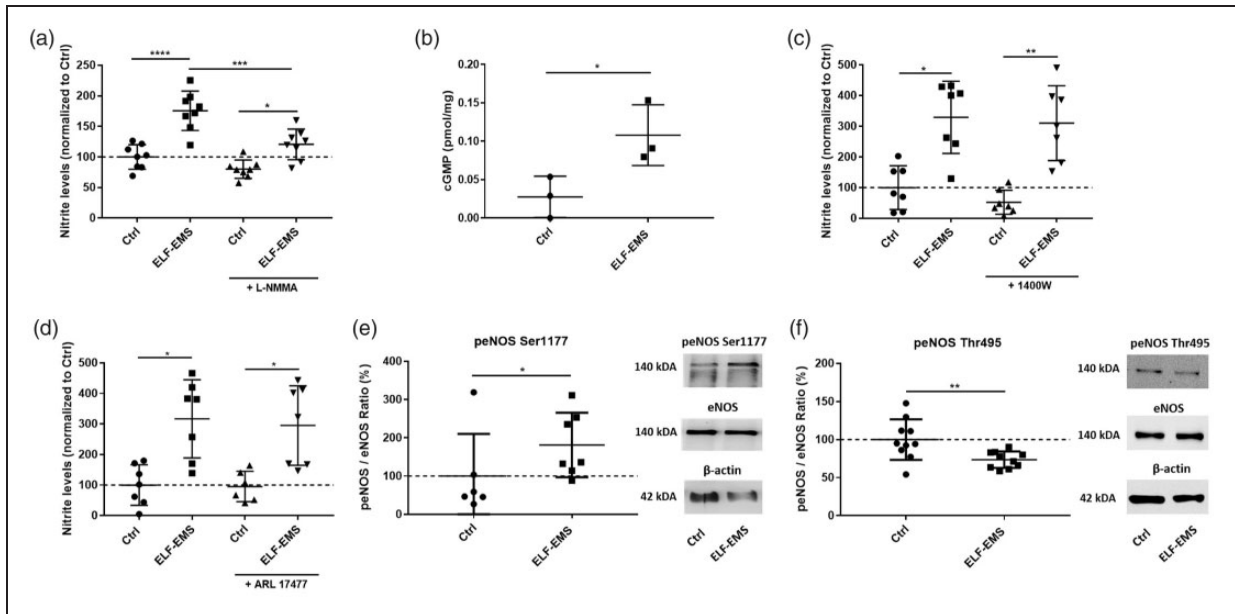


**Figure 2.** ELF-EMS increases NO production in HMEC-1 via enhanced eNOS activation. HMEC-1 were either left unstimulated or stimulated by ELF-EMS (13.5 mT, 60 Hz) for 20 min. Cells were either immediately lysed after ELF-EMS for cGMP determination and western blot analysis or were incubated for an additional 24 h to collect medium to analyze NO production via Griess assay. (a) ELF-EMS enhanced nitrite levels ( $n = 8$ ;  $p < 0.0001$ ) in HMEC-1, which could be inhibited by the pan-NOS inhibitor L-NMMA (1.5 mM) ( $n = 8$ ;  $p = 0.0005$ ). (b) cGMP concentrations were normalized to the protein concentration of each individual sample. cGMP production was increased in response to ELF-EMS ( $n = 3$ ;  $p = 0.05$ ). (c) iNOS inhibition by 1400 W (3  $\mu$ M) ( $n = 7$ ) or (d) incubation with the nNOS inhibitor ARL 17477 (5  $\mu$ M) did not affect ELF-EMS-induced nitrite production ( $n = 6$ ). (e) Quantification and representative blots of peNOS Ser117, eNOS, and  $\beta$ -actin protein levels in untreated and ELF-EMS-treated HMEC-1. The ratio of phosphorylated eNOS at Ser117 to total eNOS levels was calculated. ELF-EMS increased eNOS phosphorylation at Ser117 ( $n = 6$ ;  $p = 0.037$ ). (f) Quantification and representative blots of peNOS Thr495, eNOS, and  $\beta$ -actin protein levels in untreated and ELF-EMS-treated HMEC-1. The ratio of phosphorylated eNOS at Thr495 to total eNOS levels was calculated. ELF-EMS decreased eNOS phosphorylation at Thr495 ( $n = 10$ ;  $p = 0.005$ ).  $\beta$ -actin was included as loading control. Data are represented as mean  $\pm$  SD and are normalized to the control group (except in Figure 1(b)). \* $P < 0.05$ ; \*\* $P < 0.01$ ; \*\*\* $P < 0.001$ ; \*\*\*\* $P < 0.0001$ .

(Figure 2(f)) in HMEC-1, overall suggesting enhanced eNOS activation. These results indicate that ELF-EMS increases NO production by stimulating eNOS activity.

### Akt activation is involved in ELF-EMS-induced eNOS signaling

Since Akt is an important regulator of eNOS phosphorylation and activation,<sup>29,30</sup> the role of Akt in the eNOS-/NO pathway triggered by ELF-EMS was examined. The levels of phosphorylated Akt on Ser473 (pAkt) were increased by 45% in ELF-EMS-treated HMEC-1 compared to unstimulated cells ( $145 \pm 64\%$  vs.  $100 \pm 92\%$ ) (Figure 3(a)). To assess whether Akt is responsible for the enhanced eNOS activation by ELF-EMS, HMEC-1 were either transfected with eNOS siRNA or pre-incubated with phosphoinositide 3-kinase (PI3K) inhibitor LY294002. In control siRNA-transfected cells, ELF-EMS treatment enhanced Akt phosphorylation compared to untreated HMEC-1 ( $219 \pm 69\%$  vs.  $100 \pm 78\%$ ). Furthermore, increased pAkt levels were observed in ELF-

EMS-treated HMEC-1 transfected with eNOS siRNA compared to unstimulated eNOS siRNA-transfected cells ( $249 \pm 80\%$  vs.  $135 \pm 47\%$ ) (Figure 3(b)), indicating that silencing eNOS did not affect ELF-EMS-induced pAkt levels. In addition, LY294002 reduced nitrite production (from  $176 \pm 32\%$  to  $142 \pm 20\%$ ) (Figure 3(c)) as well as eNOS phosphorylation at Ser117 (from  $176 \pm 56\%$  to  $115 \pm 26\%$ ) (Figure 3(d)) in ELF-EMS-stimulated HMEC-1. Together, these findings indicate that Akt is an important upstream kinase responsible for ELF-EMS-induced eNOS activation.

### ELF-EMS treatment stimulates blood perfusion in the hind limb of healthy mice via activation of the Akt/eNOS pathway

eNOS-derived NO is known to regulate vascular tone by relaxing smooth muscle cells of the *tunica media*, thereby locally increasing blood flow.<sup>31</sup> Since ELF-EMS activates the Akt-/eNOS-/NO pathway *in vitro*, the effect of ELF-EMS on blood perfusion in the hind

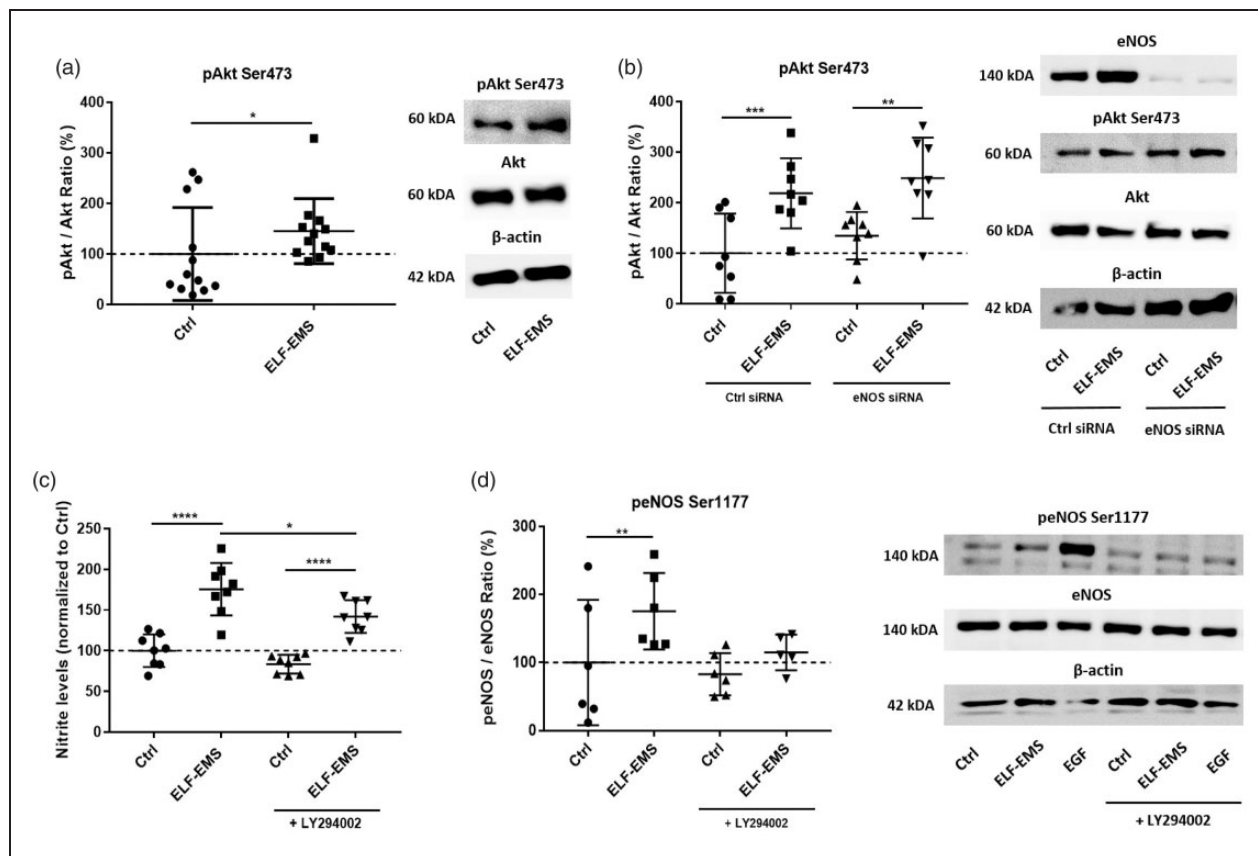


**Figure 3.** Enhanced Akt activation by ELF-EMS stimulates eNOS signaling in HMEC-I. HMEC-I were either left unstimulated or stimulated by ELF-EMS (13.5 mT, 60 Hz) for 20 min. Cells were either immediately lysed after ELF-EMS for western blot analysis or were incubated for an additional 24 h to collect medium to analyze nitrite production via Griess assay. (a) Quantification and representative blots of pAkt Ser473, Akt, and  $\beta$ -actin protein levels in untreated and ELF-EMS-treated HMEC-I. The ratio of phosphorylated Akt at Ser473 to total Akt levels was calculated. ELF-EMS enhanced Akt phosphorylation at Ser473 ( $n = 12$ ;  $p = 0.026$ ). (b) HMEC-I were transfected with non-targeting control siRNA or eNOS siRNA (both 50 nM). After 72 h of incubation, cells were either left unstimulated or stimulated by ELF-EMS. Quantification and representative blots of eNOS, pAkt Ser473, Akt, and  $\beta$ -actin protein levels in untreated and ELF-EMS-treated HMEC-I. The ratio of phosphorylated Akt at Ser473 to total Akt levels was calculated. eNOS silencing did not affect ELF-EMS-induced pAkt levels ( $n = 8$ ;  $p = 0.009$ ). (c) Treatment with LY294002 (20  $\mu$ M) reduced nitrite concentration in HMEC-I that received ELF-EMS ( $n = 8$ ;  $p = 0.016$ ). (d) Quantification and representative blots of peNOS Ser1177, eNOS, and  $\beta$ -actin protein levels in unstimulated and ELF-EMS-stimulated HMEC-I. The ratio of phosphorylated eNOS at Ser1177 to total eNOS levels was calculated. Stimulation with EGF (500 ng/ml) was included as positive control. Phosphorylation of eNOS (Ser1177) following ELF-EMS was reduced in LY294002-treated HMEC-I ( $n = 6$ ).  $\beta$ -actin was included as loading control. Data are represented as mean  $\pm$  SD and are normalized to the control group. \* $P < 0.05$ ; \*\* $P < 0.01$ ; \*\*\* $P < 0.001$ ; \*\*\*\* $P < 0.0001$ .

limbs of healthy mice was studied. This hind limb model was the preferred choice to study the effect of ELF-EMS on vascular tone since it allows to measure alterations in blood flow in a non-invasive and relatively simple and straight-forward manner using Laser Doppler flowmetry. Vascular perfusion was assessed before (as baseline) and immediately after ELF-EMS or sham treatment. Laser Doppler imaging revealed a rise of 20% in blood flow in the hind limbs that were treated with ELF-EMS compared to sham-treated hind limbs ( $120 \pm 10\%$  vs.  $100 \pm 6\%$ ) (Figure 4(a) and (b)).

To validate that the induced blood flow by ELF-EMS is due to enhanced Akt-/eNOS-/NO signaling, the effect of ELF-EMS treatment on hind limb perfusion was also assessed in the presence of NOS inhibitors. The pan-NOS inhibitor L-NAME, the nNOS inhibitor ARL 17477 and the iNOS inhibitor 1400 W were used to evaluate which NOS isoform is responsible for ELF-EMS-induced effects on blood perfusion. To assess the effect of systemic (i)NOS inhibition on NO production *in vivo*, circulating heme-nitrosylated hemoglobin (Hb-NO) levels were measured, as previously described,<sup>32</sup> in venous blood of L-NAME- and

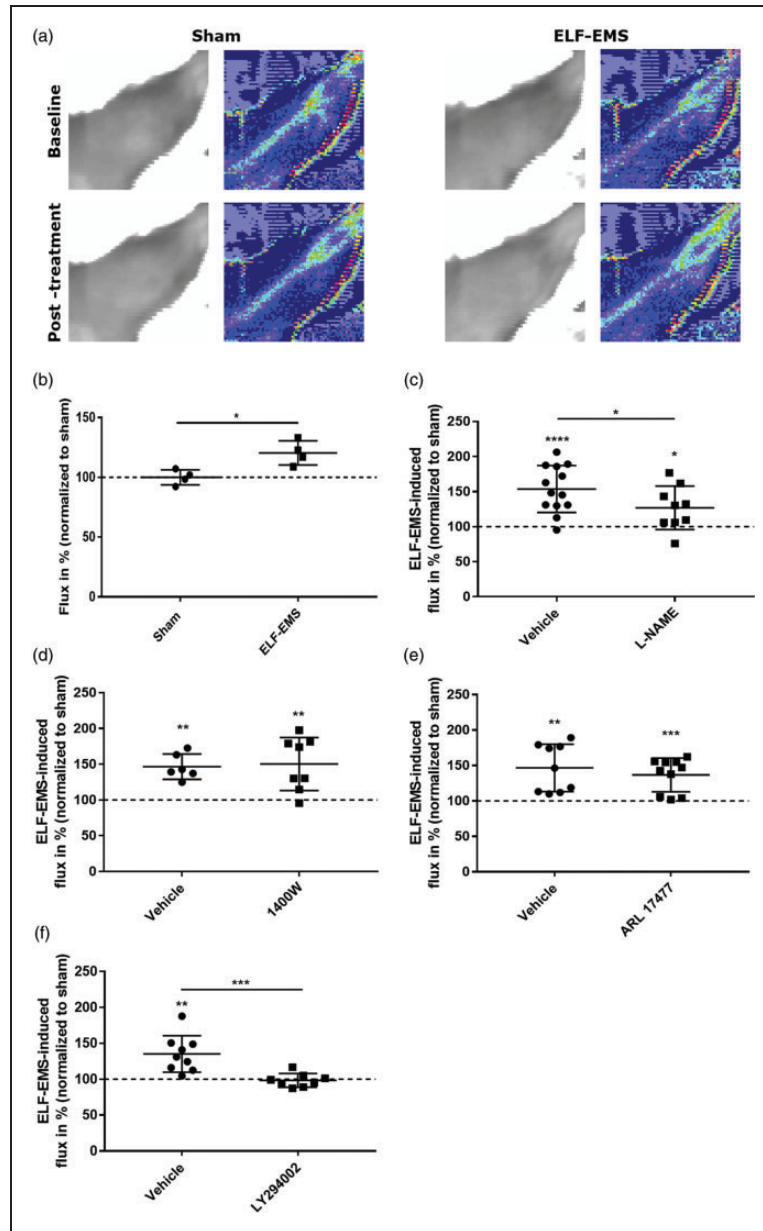


**Figure 4.** ELF-EMS application enhances vascular perfusion in the hind limb of healthy mice by activating the Akt-eNOS pathway. (a) Representative images of blood perfusion maps obtained by Laser Doppler imaging of either sham or ELF-EMS-treated hind limbs. Colored pixels illustrate blood flow variations from minimal (dark blue) to maximal (red) values. Baseline images of the blood flow were acquired before the start of either sham or ELF-EMS treatment. Post-treatment images were obtained immediately after 20 min of sham or ELF-EMS application. (b) Quantification of the blood flow from the relative flux units in the perfusion maps. ELF-EMS induced blood flow in the hind limb of healthy mice ( $n = 4$ ;  $p = 0.014$ ). (c) Mice received either vehicle or L-NAME (1 g/500 ml) in the drinking water for 5 consecutive days. Quantification of the blood flow from the relative flux units in the perfusion maps. L-NAME treatment reduced the effects of ELF-EMS on blood perfusion. ( $n = 9$ ;  $p = 0.036$ ). (d) Mice were injected with either vehicle or 1400 W (10 mg/kg) IP for 6 consecutive days. Quantification of the blood flow from the relative flux units in the perfusion maps. iNOS inhibition by 1400 W did not influence ELF-EMS-induced vascular perfusion in the hind limb ( $n = 6$ ). (e) Mice received either vehicle or ARL 17477 IP injections (10 mg/kg) for 6 consecutive days. Quantification of the blood flow from the relative flux units in the perfusion maps. Treatment of mice with ARL 17477 did not affect blood flow induced by ELF-EMS stimulation ( $n = 9$ ). (f) Mice were treated (IP) with either vehicle or LY294002 (10 mg/kg) for 3 consecutive days. Quantification of the blood flow from the relative flux units in the perfusion maps. Inhibition of the Akt pathway by LY294002 blocked ELF-EMS-mediated effects on blood perfusion in the hind limb ( $n = 8$ ;  $p = 0.0008$ ). Data are represented as mean  $\pm$  SD and are normalized to the sham-treated group. \* $P < 0.05$ ; \*\* $P < 0.01$ ; \*\*\* $P < 0.001$ ; \*\*\*\* $P < 0.0001$ .



1400 W-treated mice (Supplementary Figure 4). Treatment of mice with the pan-NOS inhibitor L-NAME reduced blood flow induction by ELF-EMS in the hind limb (from  $154 \pm 33\%$  to  $127 \pm 31\%$ ) (Figure 4(c)). In contrast, inhibition of iNOS (Figure 4(d)) or nNOS (Figure 4(e)) did not alter ELF-EMS-induced perfusion of the hind limb, suggesting that the effects of ELF-EMS on vascular perfusion are mediated by eNOS activation. Furthermore, ELF-EMS did not induce iNOS or nNOS expression in the femoral arteries of vehicle-treated mice (Supplementary Figure 3(b)), confirming that eNOS is the sole isoform responsible for ELF-EMS-induced effects. Involvement of the PI3K-/Akt pathway was investigated by treating the mice with PI3K inhibitor LY294002. LY294002 reduced the effects of ELF-EMS on blood perfusion in the hind limb (from  $135 \pm 25\%$  to  $98 \pm 10\%$ ) (Figure 4(f)). Overall, these data indicate that ELF-EMS-induced blood perfusion in the mouse hind limb depends on enhanced Akt-/eNOS-/NO signaling. Of note, baseline perfusion in the hind limb was not altered by treating the mice with either L-NAME, 1400 W, ARL 17477 or LY294002 (Supplementary Table 3). Representative perfusion images of hind limbs of mice treated with pathway inhibitors are depicted in Supplementary Figure 5.

#### *ELF-EMS increases cerebral vascular perfusion via NOS signaling in healthy collateral-rich C57BL/6 mice, but does not affect cerebral blood flow in collateral-sparse BALB/c mice*

Since the protective effect of ELF-EMS was only observed in collateral-rich C57BL/6, but not in collateral-sparse BALB/c dMCAO mice (Figure 1), and ELF-EMS induced vascular perfusion in the hind limb (Figure 4), we investigated whether ELF-EMS could increase cerebral (collateral) perfusion. In the first set of experiments, the effect of ELF-EMS on cerebral blood flow was compared in healthy C57BL/6 and BALB/c mice using LSCI. C57BL/6 mice that received ELF-EMS demonstrated an increase in cerebral blood flow by 19% compared to sham-stimulated animals ( $119 \pm 12\%$  vs.  $100 \pm 6\%$ ) (Figure 5(a) and (b)). However, ELF-EMS treatment did not augment cerebrovascular perfusion in BALB-c mice ( $105 \pm 21\%$  vs.  $100 \pm 23\%$ ) (Figure 5(c) and (d)), suggesting that the improvement in cerebral blood flow observed following ELF-EMS application is primarily the result of the recruitment of the collateral circulation.

To study the involvement of NO signaling, cerebral blood flow measurements were performed in healthy C57BL/6 mice pre-treated with the pan-NOS inhibitor L-NAME. Inhibiting NOS signaling by L-NAME

significantly diminished ELF-EMS-induced cerebrovascular perfusion in healthy C57BL/6 mouse brains ( $133 \pm 11\%$  vs.  $110 \pm 7\%$ ) (Figure 6(a)-(b)). These results indicate that ELF-EMS augments cerebral blood flow by stimulating NO signaling.

#### *ELF-EMS improves cerebral blood flow following experimental stroke*

Finally, the response of ELF-EMS on cerebrovascular perfusion was also examined in the dMCAO stroke model. Mice subjected to experimental stroke received either sham or ELF-EMS treatment for 2 days. Cerebral blood flow was measured 1 h and 24 h after dMCAO in the contralateral and ipsilateral hemispheres individually. In accordance with the data obtained in healthy brain, ELF-EMS stimulated cerebral vascular perfusion in the contralateral hemisphere of the ischemic brain both 1 h ( $127 \pm 10\%$  vs.  $100 \pm 14\%$ ) (Figure 7(a) and (c)) and 24 h ( $145 \pm 28\%$  vs.  $100 \pm 12\%$ ) (Figure 7(d) and (f)) following ischemic stroke. Comparable increases in cerebral blood flow were observed in the ischemic ipsilateral hemisphere of ELF-EMS-treated mice 1 h ( $124 \pm 14\%$  vs.  $100 \pm 8\%$ ) (Figure 7(a) and (b)) as well as 24 h ( $127 \pm 15\%$  vs.  $100 \pm 5\%$ ) (Figure 7(d) and (e)) after dMCAO.

## **Discussion**

In this study, we demonstrate that ELF-EMS improves stroke lesion volume by stimulating cerebral collateral perfusion, most likely by enhancing Akt-/eNOS-/NO signaling. Following the onset of acute ischemic stroke, the ability of collateral recruitment is a strong predictor of stroke prognosis and response to recanalization therapy.<sup>2</sup> "Collateral therapeutics", which aim to stimulate pial collateral blood flow to maintain blood supply to the penumbral tissue, hold great clinical promise to reduce ischemia-induced brain damage. In recent years, several strategies have been investigated to increase collateral perfusion after cerebral ischemia. One of the putative approaches is by targeting vasodilation of the cerebral arterioles.<sup>33</sup> Since NO is a potent vasodilator and a critical mediator in regulating cerebral blood flow, multiple research groups have investigated the use of pharmacological agents to increase post-ischemic NO content in the brain. In particular, L-arginine (a precursor of NO) and NO donors have been evaluated in animal and clinical studies.<sup>34-37</sup> Despite encouraging results in preclinical settings, application of these drugs failed in clinical trials.<sup>34,35,37,38</sup> A possible explanation for the failure of systemic administration of NO donors is the decrease in arterial blood pressure and impairment of endogenous NO production that occurs.<sup>33,39</sup> For these

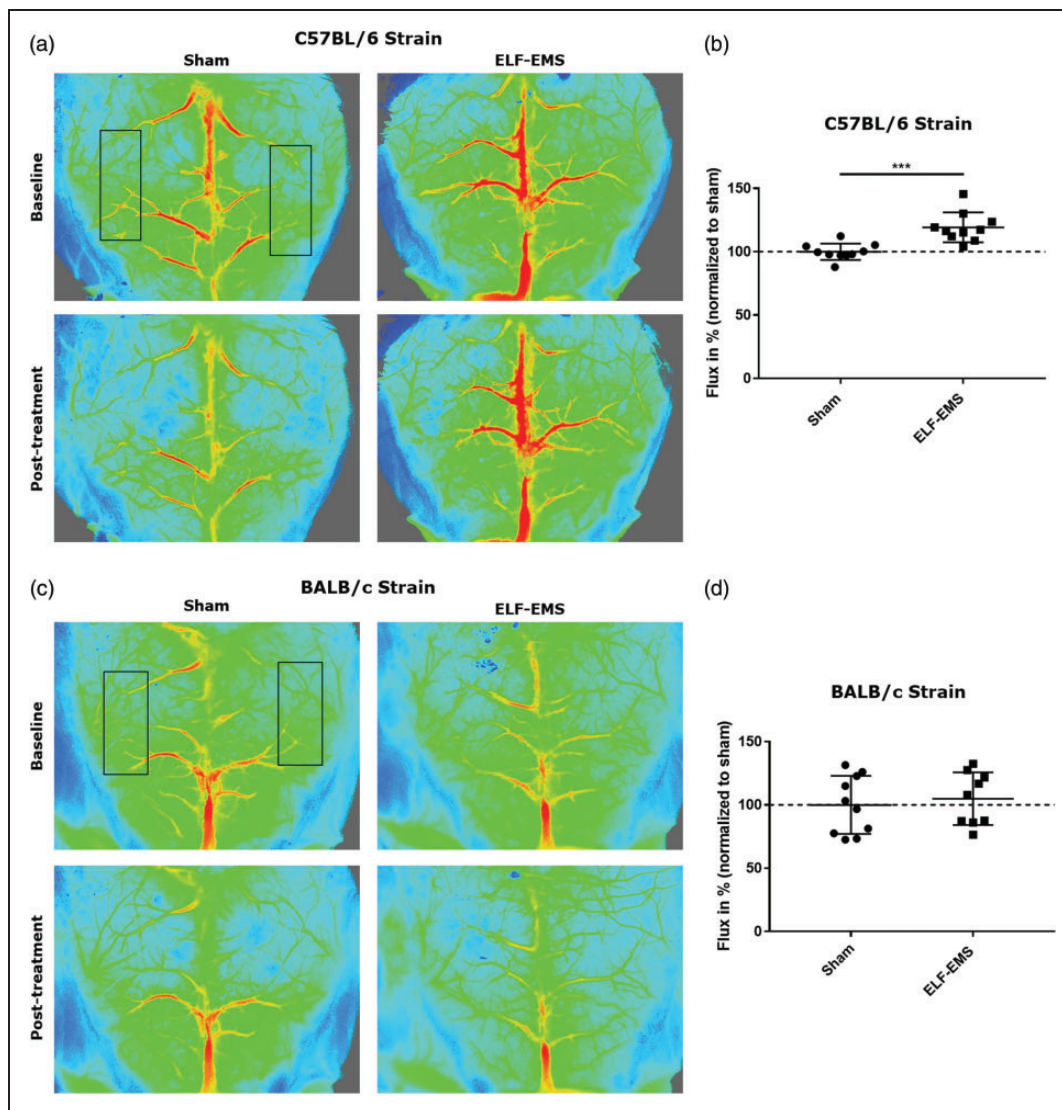


**Figure 5.** ELF-EMS augments cerebral blood flow in healthy C57BL/6 mouse brains, but did not affect cerebrovascular perfusion in BALB/c mice. (a) Representative color-coded flux images of the cerebral cortex obtained by Laser Speckle Contrast imaging of sham- or ELF-EMS-treated C57BL/6 mice. Colored pixels illustrate blood flow variations from minimal (dark blue) to maximal (red) values. Black boxes indicate the ROIs used for the measurement of blood fluxes. Baseline images of cerebral blood flow were acquired before the start of either sham or ELF-EMS treatment. Post-treatment images were obtained immediately after 20 min of sham or ELF-EMS application. (b) Quantification of the cerebral blood flow from relative flux units in the speckle images. The means of the flux values obtained from both ROIs were calculated for each image. Application of ELF-EMS increased cerebral perfusion in healthy C57BL/6 mice compared to sham treatment ( $n = 10$ ;  $p = 0.0001$ ). (c) Representative color-coded flux images of the cerebral cortex obtained by Laser Speckle Contrast imaging of sham- or ELF-EMS-treated BALB/c mice. Black boxes indicate the ROIs used for the measurement of blood fluxes. (d) Quantification of the cerebral blood flow from relative flux units in the speckle images. ELF-EMS treatment did not augment cerebrovascular perfusion in healthy BALB/c mice ( $n = 9$ ). Data are represented as mean  $\pm$  SD and are normalized to the sham-treated group. \*\*\* $p < 0.001$ .

reasons, collateral treatment strategies should aim to specifically dilate the cerebral collateral vasculature.<sup>1</sup> An advantage of ELF-EMS compared to NO donors is that it might locally induce NO production, thereby preventing unwanted systemic side effects.

Although the interest in the use of ELF-EMS in the treatment of different disorders has substantially

increased over the last couple of years, the cellular and molecular mechanisms targeted by ELF-EMS have not been fully elucidated yet. However, several reports have indicated ELF-EMS to exert its effects by modulating the NO signaling cascade.<sup>13,18–21</sup> Previous work of our research group revealed that the protective effects of ELF-EMS on stroke outcome

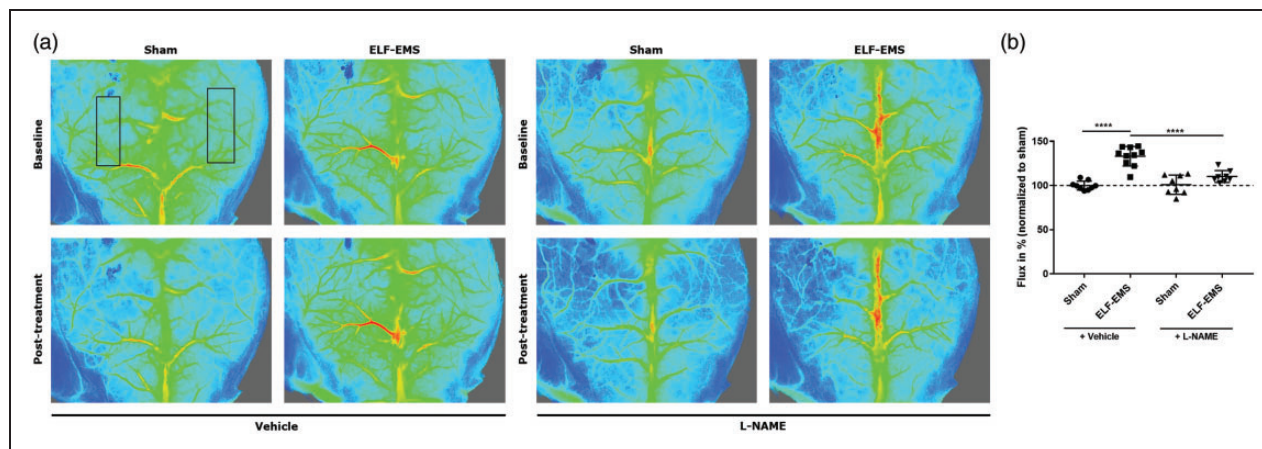


**Figure 6.** Inhibition of NOS signaling reduces ELF-EMS-induced cerebral blood flow. (a) Representative color-coded flux images of the cerebral cortex obtained by Laser Speckle Contrast imaging of sham- or ELF-EMS-treated C57BL/6 mice. Mice were pre-treated with either vehicle or L-NAME (1 g/500 ml) in the drinking water for 5 consecutive days. Colored pixels illustrate blood flow variations from minimal (dark blue) to maximal (red) values. Black boxes indicate the ROIs used for the measurement of blood fluxes. Baseline images of cerebral blood flow were acquired before the start of either sham or ELF-EMS treatment. Post-treatment images were obtained immediately after 20 min of sham or ELF-EMS application. (b) Quantification of the cerebral blood flow from relative flux units in the speckle images. L-NAME treatment inhibited ELF-EMS-induced cerebrovascular perfusion in healthy C57BL/6 mouse brains. Data are represented as mean  $\pm$  SD and are normalized to the sham-treated group ( $n = 8$ ;  $p < 0.0001$ ). \*\*\*\* $p < 0.0001$ .

in a global cerebral ischemia rat model were reverted when animals were treated with a pan-NOS inhibitor L-NAME.<sup>13</sup> Accordingly, Bragin et al. demonstrated that systemic inhibition of all NOS isoforms diminished the effects of pulsed ELF-EMS on cerebrovascular perfusion and metabolism in healthy rat brain.<sup>19</sup> Following exposure to ELF-EMS, increased NO concentrations were measured in different brain regions, including the cortex.<sup>20,40</sup> Despite several studies suggesting that ELF-EMS stimulates NO production in a NOS-dependent manner, only a few reports have tried to elucidate which NOS isoform can be held accountable for ELF-EMS-induced NO signaling. In human keratinocytes, ELF-EMS induced NO production by stimulating the expression and activity of iNOS and eNOS.<sup>18</sup> Furthermore, pulsed ELF-EMS promoted the phosphorylation of eNOS at Ser1177 in human umbilical vein endothelial cells (HUVECs) and in the ischemic muscle of mice subjected to hind limb ischemia.<sup>21</sup> Nevertheless, none of these studies assessed the direct role of the different NOS isoforms in ELF-EMS-induced NO production and vasodilation. In this study, we show that eNOS is the sole isoform responsible for the enhanced NO levels by ELF-EMS. An important consideration should be that ELF-EMS application may have distinctive effects on NO production and NOS expression/activation depending on the exposure parameters. Hence, it would be interesting to study the effect of ELF-EMS on eNOS-/NO signaling in relation to the duration, frequency, mode (pulsed

versus non-pulsed), and intensity of the generated magnetic field.

eNOS activation is tightly controlled by complex regulatory mechanisms that include positive regulation by association with post-translational proteins and through phosphorylation on different amino acid residues by various kinases.<sup>41</sup> Here, we demonstrate that ELF-EMS enhances eNOS activity by stimulating the PI3K-/Akt pathway, which is known to be responsible for eNOS phosphorylation at Ser1177.<sup>29,41</sup> However, one of the unsolved research questions remains how ELF-EMS can alter biochemical and biophysical cascades to mediate its cellular effects. ELF-EMS has shown to affect intracellular signal cascades by modulating the phosphorylation state of signaling kinases such as Akt, MEK and ERK.<sup>21,42–44</sup> Numerous studies suggested that ELF-EMS therapy could influence such signal transduction pathways by modulating ion transport and receptor binding.<sup>45</sup> In this context, several receptors have been identified to be responsible for PI3K-/Akt signaling in different cell types, including G protein-coupled receptors (GPCRs), which are a large class of transmembrane proteins accountable for signal transduction across the plasma membrane. Through the activation of numerous effector molecules, GPCRs, such as the bradykinin, adenosine and endothelin-1 receptors, effectively activate the PI3K-/Akt pathway.<sup>46,47</sup> Since ELF-EMS modulates inflammatory pain by influencing GPCR-mediated signal transduction,<sup>48</sup> it could be suggested that ELF-



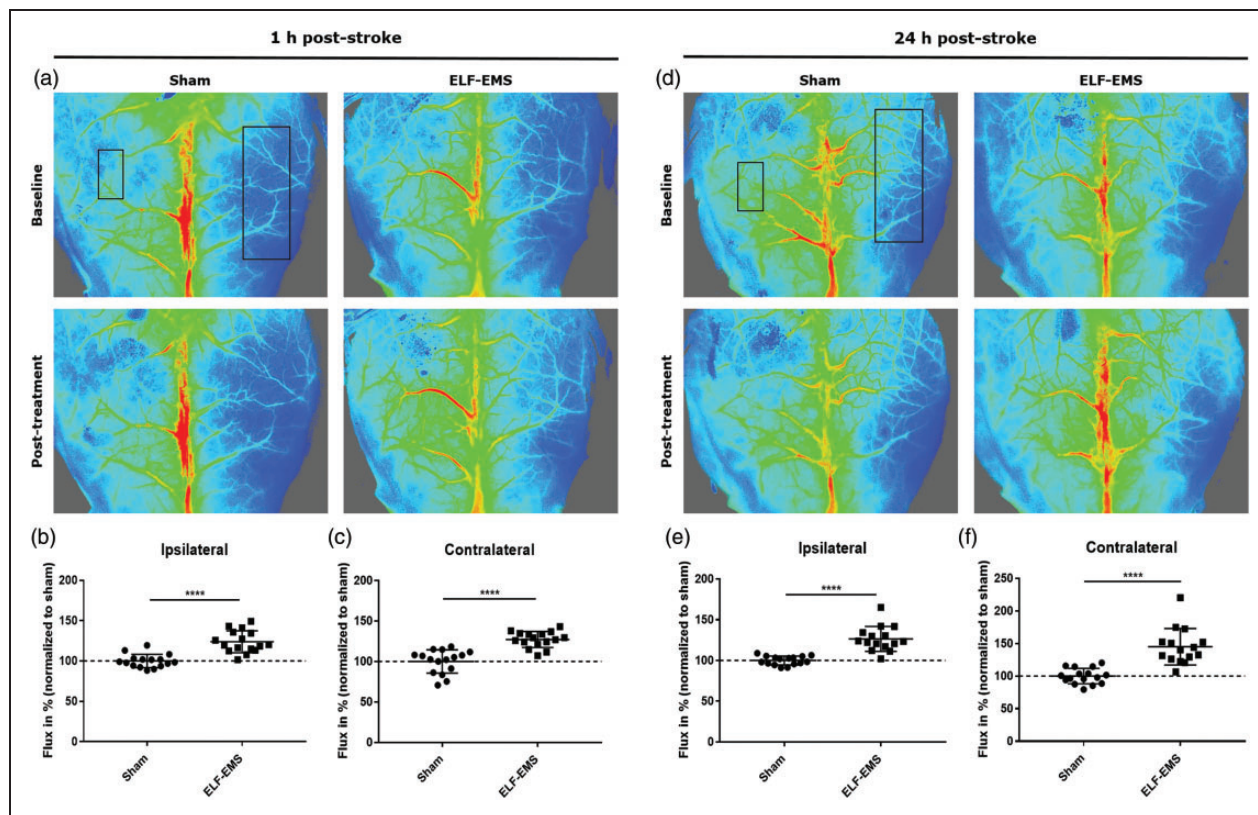


**Figure 7.** ELF-EMS increases cerebral vascular perfusion after ischemic stroke. Baseline images of cerebral blood flow were acquired before the start of either sham or ELF-EMS treatment. Post-treatment images were obtained immediately after 20 min of sham or ELF-EMS application. Colored pixels illustrate blood flow variations from minimal (dark blue) to maximal (red) values. (a) Representative color-coded flux images of the cerebral cortex obtained by Laser Speckle Contrast imaging of either sham or ELF-EMS-treated mice 1 h after dMCAO. Black boxes indicate the ROIs used for the measurement of blood fluxes. (b) Quantification of the cerebral blood flow from relative flux units in the ipsilateral hemispheres and (c) in the contralateral hemispheres 1 h following ischemic stroke. ELF-EMS treatment enhanced cerebral blood flow in both hemispheres of mice subjected to experimental stroke ( $n = 16$ ;  $p < 0.0001$ ). (d) Representative color-coded flux images of the cerebral cortex obtained by Laser Speckle Contrast imaging of either sham or ELF-EMS-treated mice 24 h following ischemic stroke. Black boxes indicate the ROIs used for blood flow measurements. (e) Quantification of the cerebral blood flow from relative flux units in the ipsilateral hemispheres and (f) in the contralateral hemispheres 24 h after stroke induction. Animals treated with ELF-EMS showed a rise in cerebrovascular perfusion in both the ipsilateral as contralateral hemispheres 24 h following dMCAO ( $n = 15$ ;  $p < 0.0001$ ). Data are represented as mean  $\pm$  SD and are normalized to the sham-treated group. \*\*\*\* $p < 0.0001$ .

EMS-induced effects on the PI3K-/Akt-/eNOS signaling pathway observed in this study are mediated by activation of a specific GPCR. Although the PI3K-/Akt pathway plays a major role in ELF-EMS-mediated eNOS phosphorylation, several other intracellular cascades could be additionally responsible for the observed effects of ELF-EMS on eNOS signaling. Indeed, early studies performed on NOS isoforms showed that eNOS is a calcium-dependent enzyme and requires calmodulin (CaM) to produce NO.<sup>49</sup> A rise in cytoplasmic calcium ( $\text{Ca}^{2+}$ ) levels increases CaM activity, which in turn binds to a canonical CaM-binding motif to displace an autoinhibitory loop on eNOS, thereby facilitating efficient NO synthesis. Application of ELF-EMS has shown to influence

intracellular and transmembrane  $\text{Ca}^{2+}$ -movements.<sup>50-52</sup> Pilla et al. demonstrated that an increase in cytoplasmic  $\text{Ca}^{2+}$  levels occurred immediately after ELF-EMS, which generates a  $\text{Ca}^{2+}$ /CaM-dependent rise in NO production.<sup>53</sup> Moreover, there is substantial evidence that ELF-EMS treatment enhances the activity of voltage-gated calcium channels (VGCCs) in numerous cell types.<sup>51,54,55</sup> By acting on VGCC function at the plasma membrane, ELF-EMS exposure could lead to increased intracellular  $\text{Ca}^{2+}$  and consequently enhanced CaM activity, thereby stimulating eNOS-dependent NO production.<sup>52</sup> Activated CaM stimulates calcium/calmodulin-dependent kinase II (CaMKII), which in turn phosphorylates eNOS on Ser1177.<sup>29</sup> Furthermore, a rise in cytosolic  $\text{Ca}^{2+}$  can



also dephosphorylate eNOS at Thr495 by stimulating the activity of  $\text{Ca}^{2+}$ -dependent phosphatases, such as calcineurin.<sup>56,57</sup> Gilbert et al. demonstrated the presence of T-type VGCCs on pulmonary endothelial cells.<sup>58</sup> Whether VGCCs are expressed in HMEC-1 warrants further investigation. Other possible targets of ELF-EMS on the endothelial plasma membrane that could lead to increased cytoplasmic  $\text{Ca}^{2+}$  levels include mechanosensitive  $\text{Ca}^{2+}$ -permeable TRPV4 channels, nonselective cation channels, and the above-mentioned GPCRs by IP3-mediated  $\text{Ca}^{2+}$  release from internal stores.<sup>59–61</sup> However, our study did not determine which upstream target(s) are responsible for the induction of the Akt/eNOS/NO pathway by ELF-EMS, which will be the subject of further investigation.

NO was discovered in the late '80s as a factor released by the endothelium causing smooth muscle relaxation and, thus, vasodilation, resulting in a local increase in vascular perfusion.<sup>62</sup> Based on evidence that ELF-EMS modulates NO signaling, several studies investigated the response of ELF-EMS application on microvascular perfusion.<sup>19,63–67</sup> In accordance with our findings, ELF-EMS has been shown to modify blood flow dynamics in the skin microvasculature of rodents and human subjects.<sup>64–67</sup> In healthy and diabetic animals exposed to hind limb ischemia, application of pulsed ELF-EMS increased blood perfusion in the wounded hind limb 14 days post-surgery compared to sham-treated animals.<sup>21,63</sup> These animals were treated daily with pulsed ELF-EMS, and the enhanced blood flow in the ischemic hind limb was presumably a result of the improved neovascularization that occurred in response to ELF-EMS. In the present study, alterations of blood perfusion in the hind limb and in the brain were measured immediately after ELF-EMS application which excludes the contribution of induced angiogenesis by ELF-EMS. Additionally, we show that ELF-EMS-induced blood flow is mediated by increased PI3K-/Akt-/eNOS signaling. In healthy rat brains, cerebral microvascular perfusion and dilation of cerebral arterioles increased immediately after pulsed ELF-EMS exposure, which gradually declined during 3 h. Inhibition of NOS by L-NAME obliterated the effects of pulsed ELF-EMS on the arterial dilation and microvascular blood flow in healthy brains, which is in accordance with our results observed in the hind limb and brains.<sup>19</sup> Nevertheless, none of these reports studied the involvement of Akt and the eNOS isoform in ELF-EMS-induced vascular perfusion.

Remarkably, in both the hind limb as well as *in vitro* experiments, pharmacological intervention of a pan-NOS inhibitor did not completely block ELF-EMS-induced effects to baseline levels. Hence, besides eNOS, additional pathways might be involved in ELF-

EMS-dependent NO synthesis and vasodilation. Firstly, the NOS-independent nitrite reduction pathway might be an alternative route responsible for NO production. Several enzymes, known as nitrite reductase proteins, can catalyze the conversion of nitrite to NO, including glutathione-S-transferases, xanthine oxidoreductase, cytochrome P450 enzymes, deoxy-hemoglobine (Hb) and deoxy-myoglobin, and components of the mitochondrial electron transport chain, such as mitochondrial cytochrome oxidase.<sup>68,69</sup> A second possibility, is that NO can be sequestered by hemes present in Hb. NO can conjugate to Cys thiols in Hb to form an S-nitrosothiol (SNO). S-nitrosohemoglobin (SNO-Hb) can locally regulate blood flow by the release of SNO from the heme group.<sup>68</sup> Whether ELF-EMS enhances the reduction of nitrite to NO or stimulates the release of SNO from Hb additional to eNOS-dependent NO synthesis, warrants further investigation.

Our research group has previously shown that ELF-EMS treatment reduced infarct size and improved functional outcome in rats subjected to global cerebral ischemia, which was likely mediated by enhanced NO signaling, since L-NAME treatment abrogated ELF-EMS-induced beneficial effects on survival and ischemic stroke volume.<sup>13</sup> Securing blood flow and oxygen supply towards the penumbra is crucial in the acute phase following ischemic stroke to minimize brain damage. The ability to recruit the leptomeningeal collateral circulation in the first hours after stroke is, therefore, a major determinant for the development of ischemia.<sup>2</sup> Based on the data obtained in the current study, we postulated that ELF-EMS could salvage penumbral tissue by inducing NO signaling in the cerebral vasculature, thereby augmenting collateral blood flow towards the hypoperfused tissue. Consistent with the effects of pulsed ELF-EMS observed on microvascular perfusion in healthy rat brain by Bragin et al.,<sup>19</sup> we show that ELF-EMS effectively increases cerebrovascular perfusion in healthy collateral-rich C57BL/6 mice, which could be blocked by inhibiting NOS signaling. Nevertheless, to our knowledge, the present study is the first to demonstrate that ELF-EMS application improves cerebral collateral blood flow in the acute stage following ischemic stroke. Multiple studies have investigated the potential of NO derivatives to stimulate cerebral perfusion as an acute treatment strategy for ischemic stroke.<sup>34,36,37</sup> A major advantage of ELF-EMS compared to these pharmacological agents is that ELF-EMS can be administered locally and non-invasively to the scalp of patients. This decreases the possibility to cause unwanted systemic side effects and excludes problems regarding the administration route and uptake through the blood-brain barrier. Because of the above-mentioned

properties, ELF-EMS could be considered as a promising therapy to bridge the critical time gap between onset/diagnosis until interventional reperfusion can occur.

To further substantiate the role for ELF-EMS in improving cerebral collateral blood flow, we evaluated the effect of ELF-EMS on cerebral perfusion and on ischemic stroke volume in two mouse strains with variations in their leptomeningeal collateral circulation. BALB/c mice possess lower numbers of cerebral collaterals in comparison with C57BL/6 mice.<sup>28</sup> In accordance, BALB/c mice displayed larger infarct volumes following dMCAO compared to C57BL/6 mice, which was inversely correlated with collateral number and diameter. Furthermore, collateral remodelling over a period of 6 days following MCAO was remarkably slower in BALB/c than in C57BL/6 mice.<sup>28</sup> In the current study, ELF-EMS reduced infarct size in C57BL/6 mice subjected to ischemic stroke, whereas ELF-EMS did not affect lesion volume in the BALB/c mouse strain. Likely, due to the fewer amount, the smaller diameter and the slower remodeling of pial collaterals in BALB/c mice, these mice did not benefit from the protective effects of ELF-EMS since it is suggested that ELF-EMS specifically dilates and stimulates cerebral collateral circuits. In accordance, ELF-EMS application did not improve cerebral blood flow in healthy collateral-scarce BALB/c mouse brains, which further indicates that the protective effects of ELF-EMS are likely mediated by enhanced recruitment of the collateral circulation. The primary limitation of the present study is that no behavioural tests were performed to assess sensorimotor recovery in response to ELF-EMS following experimental stroke. However, as reviewed by Rosell et al., no robust evidence is available on the use of specific functional tests to determine long-term functional outcome following dMCAO in mice.<sup>70</sup> Another important limitation is that the studied population of animals only included young male mice. Male mice are often the preferred sex to study new therapeutic approaches for ischemic stroke, since female animals are known to exhibit smaller infarct volumes due to the neuroprotective and vasodilatory effects of estrogen.<sup>71-73</sup> Furthermore, female endothelial cells contain higher eNOS protein levels and display greater enzymatic activity compared to male endothelial cells.<sup>74</sup> On one hand, the increased eNOS protein levels observed in female endothelium could lead to enhanced eNOS/NO signaling by ELF-EMS, thereby resulting in greater effects on cerebrovascular perfusion. On the other hand, the higher endogenous eNOS phosphorylation/activity in female endothelial cells may possibly render ELF-EMS therapy less effective to induce dilation of the female cerebral vasculature. However, whether ELF-EMS could potentially

improve cerebral collateral blood flow in females must be the subject of further investigation. Since ischemic stroke is a disease of aging, assessing the therapeutic response of ELF-EMS in aged animals will tremendously aid the translation of this 'electroceutical' into the clinic. Aging is known to influence cerebral collateral function and is associated with reduced endothelial-derived NO production often due to increased oxidative degradation or decreased vascular eNOS activity.<sup>75,76</sup> Stimulating eNOS activity and limiting NO breakdown by ROS in the aged vasculature have been considered to be attractive therapeutic options to reduce vascular dysfunction associated with advancing age.<sup>76</sup> Treatment strategies, such as estrogen or resveratrol supplementation, shown to increase eNOS expression and activation, have been reported to restore endothelial-dependent vasodilation in old animals.<sup>77-79</sup> Hence, collateral therapeutics, such as ELF-EMS, that enhance eNOS activation and thereby preserve collateral flow might be of particular interest for stroke patients.

Although this study provides strong evidence that ELF-EMS induces collateral perfusion in the brain, it cannot be excluded that other additional mechanisms could participate in the improved lesion sizes observed following dMCAO. Besides increasing Akt signaling in vascular cells, enhanced activation of this pro-survival signaling pathway in neuronal cells could be additionally responsible for the neuroprotective effects of ELF-EMS observed following experimental stroke. In a photothrombotic stroke model, Urnukhsaikhan et al. demonstrated that application of pulsed ELF-EMS reduced infarct volume and improved motor outcome, which was accompanied with increased brain-derived neurotrophic factor (BDNF) and phosphorylated Akt protein levels within the ischemic brain.<sup>43</sup> Furthermore, several reports have shown that ELF-EMS reduces post-stroke inflammation and oxidative stress, which could be responsible for the observed amelioration in stroke outcome.<sup>12,43,80</sup> In addition, ELF-EMS promoted neuroplasticity and increased hippocampal neurogenesis in rats subjected to cerebral ischemia.<sup>81,82</sup> The current study did not investigate possible additional mechanisms activated by ELF-EMS following stroke (*i.e.* direct neuroprotective effects on neurons) and should be the subject of further investigation. The potential of ELF-EMS to induce cerebral collateral perfusion in the acute phase, and even its reported (but not investigated in this study) beneficial effects on inflammation and neuroregeneration in the sub-acute/chronic phases holds great clinical promise for ELF-EMS as a treatment for ischemic stroke patients.

In conclusion, we show that ELF-EMS enhances Akt-/eNOS-/NO signaling in a human endothelial cell line, and activation of this pathway is responsible for

ELF-EMS-induced vascular perfusion observed in the hind limb of healthy mice. Additionally, ELF-EMS stimulates cerebral collateral blood flow in the ischemic brain, thereby reducing brain damage following ischemic stroke. Our unprecedented findings suggest that ELF-EMS is a promising therapeutic approach for the treatment of ischemic stroke by improving collateralization. A major advantage of this potential stroke therapy is that ELF-EMS is already applied in the clinic for the treatment of several conditions, such as postoperative pain, edema, and chronic wounds, which will aid its clinical translation. Future studies should focus on assessing the optimal treatment protocol, magnetic flux density and spatial distribution of ELF-EMS in the injured tissue to achieve maximal desired therapeutic effects.

### Funding

The author(s) disclosed receipt of the following financial support for the research, authorship, and/or publication of this article: This research is supported by the ‘Special Research Funds’ (BOF) of Hasselt University (grants # BOF20TT04 and 18NI06BOF to Annelies Bronckaers and Hannelore Kemps). At UCLouvain, this study was supported by the Fonds National de la Recherche Scientifique (F.R.S.-FNRS, grants # J.0111.17F to Chantal Dessy, and grants # 1.5.141.06 and 1.B181.08 to Pierre Sonveaux). Chantal Dessy and Pierre Sonveaux are Senior Research Associate and Research Director of the F.R.S.-FNRS respectively. Robin Lemmens is a senior clinical investigator of Fonds Wetenschappelijk Onderzoek (FWO) Flanders.

### Acknowledgements

The authors would like to send out a word of gratitude to Marc Jans, Evelyne Van Kerckhove, Jeanine Santermans, Thibaut Vazeille, Rachid El Kaddouri, Tim Vangansewinkel, and Laura Ponsaerts for their excellent technical assistance.

### Declaration of conflicting interests

The author(s) declared no potential conflicts of interest with respect to the research, authorship, and/or publication of this article.

### Authors' contributions

Hannelore Kemps, Bert Brône, Robin Lemmens and Annelies Bronckaers participated in the study design, data interpretation and coordination of the project. Hannelore Kemps carried out the *in vitro* and *in vivo* experiments and participated in data collection, analysis as well as data interpretation and manuscript writing. Chantal Dessy was involved in the study design of the *in vivo* experiments. Chantal Dessy, Laurent Dumas, Lotte Alders, Jana Van Broeckhoven, Sara Lambrechts and Sébastien Foulquier assisted in *in vivo* experiments, data analysis, and interpretation. Lena Perez Font designed the ELF-EMS equipment.

Pierre Sonveaux and Sven Hendrix were involved in data interpretation and reviewed the manuscript. Annelies Bronckaers supervised the experiments and helped to draft the final manuscript. All authors have revised and approved the final version of the manuscript.

### ORCID iD

Bert Brône  <https://orcid.org/0000-0002-4851-9480>

### Supplemental material

Supplemental material for this article is available online.

### References

1. Liu J, Wang Y, Akamatsu Y, et al. Vascular remodeling after ischemic stroke: mechanisms and therapeutic potentials. *Prog Neurobiol* 2014; 115: 138–156.
2. Christoforidis GA, Mohammad Y, Kehagias D, et al. Angiographic assessment of pial collaterals as a prognostic indicator following intra-arterial thrombolysis for acute ischemic stroke. *AJNR Am J Neuroradiol* 2005; 26: 1789–1797.
3. Terpolilli NA, Moskowitz MA and Plesnila N. Nitric oxide: considerations for the treatment of ischemic stroke. *J Cereb Blood Flow Metab* 2012; 32: 1332–1346.
4. MacMicking J, Xie QW and Nathan C. Nitric oxide and macrophage function. *Annu Rev Immunol* 1997; 15: 323–350.
5. Zhang RL, Zhang ZG and Chopp M. Targeting nitric oxide in the subacute restorative treatment of ischemic stroke. *Expert Opin Investig Drugs* 2013; 22: 843–851.
6. Garry PS, Ezra M, Rowland MJ, et al. The role of the nitric oxide pathway in brain injury and its treatment – from bench to bedside. *Exp Neurol* 2015; 263: 235–243.
7. Hsu YC, Chang YC, Lin YC, et al. Cerebral microvascular damage occurs early after hypoxia-ischemia via nNOS activation in the neonatal brain. *J Cereb Blood Flow Metab* 2014; 34: 668–676.
8. Chen J, Zacharek A, Zhang C, et al. Endothelial nitric oxide synthase regulates brain-derived neurotrophic factor expression and neurogenesis after stroke in mice. *J Neurosci* 2005; 25: 2366–2375.
9. Luo CX, Zhu XJ, Zhou QG, et al. Reduced neuronal nitric oxide synthase is involved in ischemia-induced hippocampal neurogenesis by up-regulating inducible nitric oxide synthase expression. *J Neurochem* 2007; 103: 1872–1882.
10. Yang Y, Li L, Wang YG, et al. Acute neuroprotective effects of extremely low-frequency electromagnetic fields after traumatic brain injury in rats. *Neurosci Lett* 2012; 516: 15–20.
11. Tasset I, Medina FJ, Jimena I, et al. Neuroprotective effects of extremely low-frequency electromagnetic fields on a Huntington's disease rat model: effects on neurotrophic factors and neuronal density. *Neuroscience* 2012; 209: 54–63.
12. Pena-Philippides JC, Yang Y, Bragina O, et al. Effect of pulsed electromagnetic field (PEMF) on infarct size and



- inflammation after cerebral ischemia in mice. *Transl Stroke Res* 2014; 5: 491–500.
13. Font LP, Cardonne MM, Kemps H, et al. Non-pulsed sinusoidal electromagnetic field rescues animals from severe ischemic stroke via NO activation. *Front Neurosci* 2019; 13: 561.
  14. Rohde C, Chiang A, Adipoju O, et al. Effects of pulsed electromagnetic fields on interleukin-1 beta and postoperative pain: a double-blind, placebo-controlled, pilot study in breast reduction patients. *Plast Reconstr Surg* 2010; 125: 1620–1629.
  15. Gossling HR, Bernstein RA and Abbott J. Treatment of ununited tibial fractures: a comparison of surgery and pulsed electromagnetic fields (PEMF). *Orthopedics* 1992; 15: 711–719.
  16. Pennington GM, Danley DL, Sumko MH, et al. Pulsed, non-thermal, high-frequency electromagnetic energy (DIAPULSE) in the treatment of grade I and grade II ankle sprains. *Mil Med* 1993; 158: 101–104.
  17. Pesce M, Patruno A, Speranza L, et al. Extremely low frequency electromagnetic field and wound healing: implication of cytokines as biological mediators. *Eur Cytokine Netw* 2013; 24: 1–10.
  18. Patruno A, Amerio P, Pesce M, et al. Extremely low frequency electromagnetic fields modulate expression of inducible nitric oxide synthase, endothelial nitric oxide synthase and cyclooxygenase-2 in the human keratinocyte cell line HaCat: potential therapeutic effects in wound healing. *Br J Dermatol* 2010; 162: 258–266.
  19. Bragin DE, Statom GL, Hagberg S, et al. Increases in microvascular perfusion and tissue oxygenation via pulsed electromagnetic fields in the healthy rat brain. *JNS* 2015; 122: 1239–1247.
  20. Cho SI, Nam YS, Chu LY, et al. Extremely low-frequency magnetic fields modulate nitric oxide signaling in rat brain. *Bioelectromagnetics* 2012; 33: 568–574.
  21. Li RL, Huang JJ, Shi YQ, et al. Pulsed electromagnetic field improves postnatal neovascularization in response to hindlimb ischemia. *Am J Transl Res* 2015; 7: 430–444.
  22. Percie Du Sert N, Hurst V, Ahluwalia A, et al. The ARRIVE guidelines 2.0: updated guidelines for reporting animal research. *J Cereb Blood Flow Metab* 2020; 40: 1769–1777.
  23. Llovera G, Roth S, Plesnila N, et al. Modeling stroke in mice: permanent coagulation of the distal middle cerebral artery. *J Vis Exp* 2014; e51729.
  24. Brouet A, DeWever J, Martinive P, et al. Antitumor effects of in vivo caveolin gene delivery are associated with the inhibition of the proangiogenic and vasodilatory effects of nitric oxide. *Faseb J* 2005; 19: 602–604.
  25. Vlahos CJ, Matter WF, Hui KY, et al. A specific inhibitor of phosphatidylinositol 3-kinase, 2-(4-morpholinyl)-8-phenyl-4H-1-benzopyran-4-one (LY294002). *J Biol Chem* 1994; 269: 5241–5248.
  26. Garvey EP, Oplinger JA, Furfine ES, et al. 1400W is a slow, tight binding, and highly selective inhibitor of inducible nitric-oxide synthase in vitro and in vivo. *J Biol Chem* 1997; 272: 4959–4963.
  27. Zhang ZG, Reif D, Macdonald J, et al. ARL 17477, a potent and selective neuronal NOS inhibitor decreases infarct volume after transient middle cerebral artery occlusion in rats. *J Cereb Blood Flow Metab* 1996; 16: 599–604.
  28. Zhang H, Prabhakar P, Sealock R, et al. Wide genetic variation in the native pial collateral circulation is a major determinant of variation in severity of stroke. *J Cereb Blood Flow Metab* 2010; 30: 923–934.
  29. Sessa WC. eNOS at a glance. *J Cell Sci* 2004; 117: 2427–2429.
  30. Govers R and Rabelink TJ. Cellular regulation of endothelial nitric oxide synthase. *Am J Physiol Renal Physiol* 2001; 280: F193–206.
  31. Levine AB, Punahaole D and Levine TB. Characterization of the role of nitric oxide and its clinical applications. *Cardiology* 2012; 122: 55–68.
  32. Desjardins F, Lobysheva I, Pelat M, et al. Control of blood pressure variability in caveolin-1-deficient mice: role of nitric oxide identified in vivo through spectral analysis. *Cardiovasc Res* 2008; 79: 527–536.
  33. Winship IR. Cerebral collaterals and collateral therapeutics for acute ischemic stroke. *Microcirculation* 2015; 22: 228–236.
  34. Bath PM, Willmot M, Leonardi-Bee J, et al. Nitric oxide donors (nitrates), L-arginine, or nitric oxide synthase inhibitors for acute stroke. *Cochrane Database Syst Rev* 2002; CD000398.
  35. Khan M, Jatana M, Elango C, et al. Cerebrovascular protection by various nitric oxide donors in rats after experimental stroke. *Nitric Oxide* 2006; 15: 114–124.
  36. Terpolilli NA, Kim SW, Thal SC, et al. Inhalation of nitric oxide prevents ischemic brain damage in experimental stroke by selective dilatation of collateral arterioles. *Circ Res* 2012; 110: 727–738.
  37. Morikawa E, Moskowitz MA, Huang Z, et al. L-arginine infusion promotes nitric oxide-dependent vasodilation, increases regional cerebral blood flow, and reduces infarction volume in the rat. *Stroke* 1994; 25: 429–435.
  38. Willmot M, Gray L, Gibson C, et al. A systematic review of nitric oxide donors and L-arginine in experimental stroke; effects on infarct size and cerebral blood flow. *Nitric Oxide* 2005; 12: 141–149.
  39. Munzel T, Li H, Mollnau H, et al. Effects of long-term nitroglycerin treatment on endothelial nitric oxide synthase (NOS III) gene expression, NOS III-mediated superoxide production, and vascular NO bioavailability. *Circ Res* 2000; 86: E7–E12.
  40. Jelenkovic A, Janac B, Pesic V, et al. Effects of extremely low-frequency magnetic field in the brain of rats. *Brain Res Bull* 2006; 68: 355–360.
  41. Dudzinski DM and Michel T. Life history of eNOS: partners and pathways. *Cardiovasc Res* 2007; 75: 247–260.
  42. Hao CN, Huang JJ, Shi YQ, et al. Pulsed electromagnetic field improves cardiac function in response to myocardial infarction. *Am J Transl Res* 2014; 6: 281–290.
  43. Urnukhsaikhan E, Mishig-Ochir T, Kim SC, et al. Neuroprotective effect of low frequency-pulsed electromagnetic fields in ischemic stroke. *Appl Biochem Biotechnol* 2017; 181: 1360–1371.



44. Sheikh AQ, Taghian T, Hemingway B, et al. Regulation of endothelial MAPK/ERK signalling and capillary morphogenesis by low-amplitude electric field. *J R Soc Interface* 2013; 10: 20120548.
45. Markov MS. Expanding use of pulsed electromagnetic field therapies. *Electromagn Biol Med* 2007; 26: 257–274.
46. Nakano N, Matsuda S, Ichimura M, et al. PI3K/AKT signaling mediated by G protein-coupled receptors is involved in neurodegenerative parkinson's disease (review). *Int J Mol Med* 2017; 39: 253–260.
47. New DC, Wu K, Kwok AW, et al. G protein-coupled receptor-induced akt activity in cellular proliferation and apoptosis. *Febs J* 2007; 274: 6025–6036.
48. Ross CL, Teli T and Harrison BS. Electromagnetic field devices and their effects on nociception and peripheral inflammatory pain mechanisms. *Altern Ther Health Med* 2016; 22: 52–64.
49. Fulton D, Gratton JP and Sessa WC. Post-translational control of endothelial nitric oxide synthase: why isn't calcium/calmodulin enough? *J Pharmacol Exp Ther* 2001; 299: 818–824.
50. Jeong JH, Kum C, Choi HJ, et al. Extremely low frequency magnetic field induces hyperalgesia in mice modulated by nitric oxide synthesis. *Life Sci* 2006; 78: 1407–1412.
51. Fanelli C, Coppola S, Barone R, et al. Magnetic fields increase cell survival by inhibiting apoptosis via modulation of Ca<sup>2+</sup> influx. *Faseb J* 1999; 13: 95–102.
52. Pall ML. Electromagnetic fields act via activation of voltage-gated calcium channels to produce beneficial or adverse effects. *J Cell Mol Med* 2013; 17: 958–965.
53. Pilla AA. Electromagnetic fields instantaneously modulate nitric oxide signaling in challenged biological systems. *Biochem Biophys Res Commun* 2012; 426: 330–333.
54. Morgado-Valle C, Verdugo-Diaz L, Garcia DE, et al. The role of voltage-gated Ca<sup>2+</sup> channels in neurite growth of cultured chromaffin cells induced by extremely low frequency (ELF) magnetic field stimulation. *Cell Tissue Res* 1998; 291: 217–230.
55. Piacentini R, Ripoli C, Mezzogori D, et al. Extremely low-frequency electromagnetic fields promote in vitro neurogenesis via upregulation of Ca(v)1-channel activity. *J Cell Physiol* 2008; 215: 129–139.
56. Harris MB, Ju H, Venema VJ, et al. Reciprocal phosphorylation and regulation of endothelial nitric-oxide synthase in response to bradykinin stimulation. *J Biol Chem* 2001; 276: 16587–16591.
57. Fleming I, Fisslthaler B, Dimmeler S, et al. Phosphorylation of thr(495) regulates Ca(2+)/calmodulin-dependent endothelial nitric oxide synthase activity. *Circ Res* 2001; 88: E68–75.
58. Gilbert G, Courtois A, Dubois M, et al. T-type voltage gated calcium channels are involved in endothelium-dependent relaxation of mice pulmonary artery. *Biochem Pharmacol* 2017; 138: 61–72.
59. Goedicke-Fritz S, Kaistha A, Kacik M, et al. Evidence for functional and dynamic microcompartmentation of cav-1/TRPV4/K(Ca) in caveolae of endothelial cells. *Eur J Cell Biol* 2015; 94: 391–400.
60. Kohler R and Hoyer J. Role of TRPV4 in the mechano-transduction of shear stress in endothelial cells. In: Liedtke WB and Heller S (eds) *TRP ion channel function in sensory transduction and cellular signaling Cascades*. Boca Raton, FL: CRC Press/Taylor & Francis, 2007.
61. Rath G, Dessy C and Feron O. Caveolae, caveolin and control of vascular tone: nitric oxide (NO) and endothelium derived hyperpolarizing factor (EDHF) regulation. *J Physiol Pharmacol* 2009; 60 Suppl 4: 105–109.
62. Ignarro LJ, Buga GM, Wood KS, et al. Endothelium-derived relaxing factor produced and released from artery and vein is nitric oxide. *Proc Natl Acad Sci U S A* 1987; 84: 9265–9269.
63. Pan Y, Dong Y, Hou W, et al. Effects of PEMF on microcirculation and angiogenesis in a model of acute hindlimb ischemia in diabetic rats. *Bioelectromagnetics* 2013; 34: 180–188.
64. Traikov L, Antonov I, Petrova J, et al. Signal processing and wavelet analysis of simultaneously registered blood pressure and laser doppler flow signals during extremely low frequency electromagnetic field exposure in humans in vivo. *Environmentalist* 2011; 31: 187–195.
65. Xu S, Okano H and Ohkubo C. Acute effects of whole-body exposure to static magnetic fields and 50-Hz electromagnetic fields on muscle microcirculation in anesthetized mice. *Bioelectrochemistry* 2001; 53: 127–135.
66. Mayrovitz H and Larsen P. Effects of pulsed magnetic fields on skin microvascular blood perfusion. *Wounds* 1992; 4: 197–202.
67. Ohkubo C and Xu S. Acute effects of static magnetic fields on cutaneous microcirculation in rabbits. *In Vivo* 1997; 11: 221–225.
68. Premont RT, Reynolds JD, Zhang R, et al. Role of nitric oxide carried by hemoglobin in cardiovascular physiology. *Circ Res* 2020; 126: 129–158.
69. Pellegrino D and Parisella ML. Nitrite as a physiological source of nitric oxide and a signalling molecule in the regulation of the cardiovascular system in both mammalian and non-mammalian vertebrates. *Recent Pat Cardiovasc Drug Discov* 2010; 5: 91–96.
70. Rosell A, Agin V, Rahman M, et al. Distal occlusion of the middle cerebral artery in mice: are we ready to assess long-term functional outcome? *Transl Stroke Res* 2013; 4: 297–307.
71. Sohrabji F, Park MJ and Mahnke AH. Sex differences in stroke therapies. *J Neurosci Res* 2017; 95: 681–691.
72. Krause DN, Duckles SP and Pelligrino DA. Influence of sex steroid hormones on cerebrovascular function. *J Appl Physiol* 2006; 101: 1252–1261.
73. McNeill AM, Zhang C, Stanczyk FZ, et al. Estrogen increases endothelial nitric oxide synthase via estrogen receptors in rat cerebral blood vessels. *Stroke* 2002; 33: 1685–1691.
74. Cattaneo MG, Vanetti C, Decimo I, et al. Sex-specific eNOS activity and function in human endothelial cells. *Sci Rep* 2017; 7: 9612–9608.
75. Ma J, Ma Y, Shuaib A, et al. Impaired collateral flow in pial arterioles of aged rats during ischemic stroke. *Transl Stroke Res* 2020; 11: 243–253.

76. Cau S, Carneiro F and Tostes R. Differential modulation of nitric oxide synthases in aging: therapeutic opportunities. *Front Physiol* 2012; 3: 218. Review.
77. LeBlanc AJ, Reyes R, Kang LS, et al. Estrogen replacement restores flow-induced vasodilation in coronary arterioles of aged and ovariectomized rats. *Am J Physiol Regul Integr Comp Physiol* 2009; 297: R1713–R1723.
78. Rajapakse AG, Yepuri G, Carvas JM, et al. Hyperactive S6K1 mediates oxidative stress and endothelial dysfunction in aging: Inhibition by resveratrol. *Plos One* 2011; 6: e19237.
79. Schmitt CA, Heiss EH and Dirsch VM. Effect of resveratrol on endothelial cell function: molecular mechanisms. *BioFactors* 2010; 36: 342–349.
80. Cichoń N, Bijak M, Miller E, et al. Extremely low frequency electromagnetic field (ELF-EMF) reduces oxidative stress and improves functional and psychological status in ischemic stroke patients. *Bioelectromagnetics* 2017; 38: 386–396.
81. Segal Y, Segal L, Blumenfeld-Katzir T, et al. The effect of electromagnetic field treatment on recovery from ischemic stroke in a rat stroke model: Clinical, imaging, and pathological findings. *Stroke Res Treat* 2016; 2016: 6941946–6941903.
82. Gao Q, Leung A, Yang YH, et al. Extremely low frequency electromagnetic fields promote cognitive function and hippocampal neurogenesis of rats with cerebral ischemia. *Neural Regen Res* 2021; 16: 1252–1257.